PERFORMANCES OF THE 3D STRAIN BASED FINITE ELEMENTS

T. MAALEM

Civil Engineering Department, University of Batna, Algeria BP 266 RP 05000 Batna-Algeria

ABSTRACT

Some of the 3D strain based finite elements are presented shortly. They have eight nodes per element, except for the condensed one, whom have nine in the departure. Each of the nodes contains the three usual d.o.f., these elements were developed not only for the study of the 3D problems but also for the analysis of thin and thick plates. Among its, one has a regular shape, indeed the SBP8element (strain based parallelepiped 8 nodes) is presented in detail. Numerical examples show that it possesses properties of high accuracy, is capable of passing the various patch tests, and does not exhibit extra zero energy modes. It is free from locking for very thin plate analysis, and has better performance compared with his "congener" the conforming displacement element and some other 3D elements.

Key words: parallelepiped elements; strain model; three-dimensional elasticity; plate bending; transverse shear locking

1 INTRODUCTION

Practice shows that the engineers prefer to model their structures with the simplest finite elements (nodes only in the corners; the same number of unknowns by node…), such quadrangles with 4 nodes or bricks with 8 nodes. However, in a state of pure bending, there is no deformation in the perpendicular direction of the median plan. Consequently, if $\nu \neq 0$, stresses originate from this direction, coming so to decrease strains in the plan. To avoid this phenomenon, one can define either for the material artificial anisotropic properties, or to use a parabolic displacement fields in all the directions, these two methods are expensive. To overcome this, 3D strain based elements were developed. Although the appearance of this model going back up to the 1970s [1, 2], the strain model was not enough investigated in the past in spite of the numerous advantages, which presents with regard to classic models. The objective of this paper is to put in evidence the power of this model and especially that of 3D strain based elements.

The success of the 2D strain based finite elements [3, 5], encouraged authors [6, 7] to develop the 3D version, contributing so to enrich the existing finite elements library. These elements were developed not only for the study of the 3D problems but also for the analysis of thin and thick plates. They allow a very good representation the transverse shear without any risk of locking [8, 12].

The behavior law is modified by the introduction of the plane stress constants and a corrective coefficient of transverse shear noted K. This method, which is underlying in Ahmad's element [13], consists in modifying the matrix of elastic constants, so as to represent with more meadows the real behavior of plates and shells, that they are thin or thick; the modification has the effect of softening the elementary stiffness matrix.

The first 3D element developed is the SBH8 [6, 7] which has a hexahedral shape; numerical examples show that it possesses properties of high accuracy. If we add to the displacement field the verification of the 3 equilibrium equations and by giving a particular shape (parallelepiped) a new element is obtained [8, 9] it has a good performance, particularly for the constraints results (moments) although, it does not improve in sensitive way the displacements results. Another 3D element was developed with a new formulation the SBBM8 [10] and always more and more successful results are obtained. Finally and with the use of the condensation concept a new 3D element is formulated [11] the SBP8C, which has a good performance [12], because of its enriched displacement field. All these elements satisfied easily the main two convergence criteria (constant strain and rigid body motion conditions), the various strain components are easily decoupled (a field of uncoupled displacements generates coupled deformations), the displacement field can be enriched by terms of high order without the introduction of intermediate nodes or supplementary d.o.f (allowing so to treat the problem of locking).

2 DESCRIPTION OF THE SBP8 ELEMENT

As example for the 3D strain based elements, this study is focused essentially on the SBP8 one, its geometry and the correspondent Kinematic variable are shown in Fig. 1In every node (i) is attributed the three d.o.f Ui, Vi and Wi

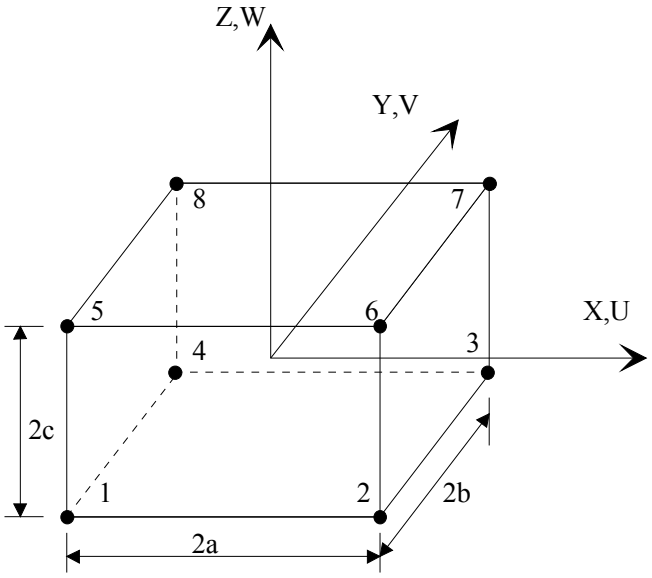

Figure1: Geometry of the SBP8 element.

3 FORMULATION OF THE SBP8 ELEMENT

3.1 Displacement field

For a linear theory where unitarian displacements are weak, there are six strain components occurring in completely 3D analysis.

The assumed strains are:

$$\varepsilon_{xx} = U_{,x} \qquad \gamma_{xy}=U_{,y}+V_{,x} \tag{1a, b}$$

$$\varepsilon_{yy} = V_{,y} \qquad \gamma yz = V_{,z} + W_{,y} \tag{1c, d}$$

$$\varepsilon_{zz} = W_{,z} \qquad \gamma xz = W_{,x} + U_{,z} \tag{1e, f}$$

U, V et W: are the displacements in the three directions X, Y et Z respectively. Equations (2) represent the condition of the rigid body motion (RBM). We have:

$$\varepsilon ii = 0 \tag{2a}$$

$$\gamma ij = 0 \tag{2b}$$

The integration of (2) allows to obtain a particular solution:

$$U_R = a_1 + a_4\, y + a_6\, z \tag{3a}$$

$$V_R = a_2 - a_4\, x - a_5\, z \tag{3b}$$

$$W_R = a_3 + a_5\, y - a_6 \tag{3c}$$

Equations (3) represent the displacement fields corresponding to the rigid body motion (RBM). The present element is an eight parallelepiped node with three degrees of freedom (d.o.f) by node (Fig.1). Therefore, the displacement field has to contain twenty-four independent constants. Six of them (a1 , a2 , ... a6) are already used to represent the RBM, it remains so eighteen (a7, a8 , ... a24) to represent in a rough way deformation in the element, while verifying the six equations of compatibility and the three equations of equilibrium. The strain field is :

$$\varepsilon_{xx} = a_7 + a_8\, y + a_9\, z + a_{10}\, yz \tag{4a}$$

$$\varepsilon_{yy} = a_{11} + a_{12}\, x + a_{13}\, z + a_{14}\, xz \tag{4b}$$

$$\varepsilon_{zz} = a_{15} + a_{16}\, x + a_{17}\, y + a_{18}\, xy \tag{4c}$$

$$\gamma_{yz} = a_{19} + a_{20}\, x - \alpha\,[\lambda/G(a_8\, z + a_{10}(z^2/2) + a_9\, y + a_{10}\,(y^2/2))] \tag{4d}$$

$$\gamma_{xz} = a_{21} + a_{22}\, y - \alpha\,[\lambda/G(a_{16}\, z + a_{14}(z^2/2) + a_{13}\, x + a_{14}\,(x^2/2))] \tag{4e}$$

$$\gamma_{xy} = a_{23} + a_{24}\, z - \alpha\,[\lambda/G(a_{12}\, y + a_{18}(y^2/2) + a_{17}\, x + a_{18}\,(x^2/2))] \tag{4f}$$

Where λ, G denote Lamé constants and α is a factor which can takes 0 or 1 values. Terms between brackets were added to satisfy the three-dimensional equilibrium equations. Substituting equations (4) into (1) and solving the resulting differential equations gives:

$$\begin{aligned} U = {} & a1 + a4\, y + a6\, z + a7\, x + a8\, xy + a9\, xz \\ & + a10\, xyz - 0.5\, a12\,(y2 + \alpha\, y2) \\ & - 0.5\, a14\,(y2z + (\alpha z3)/3) - 0.5\, a16(\, z2 + \alpha\, z2) \\ & - 0.5\, a18(\, yz2 + (\alpha y3)/3) + 0.5\, a21\, z \\ & + 0.5\, a23\, y + a24\, yz \end{aligned} \tag{5a}$$

$$\begin{aligned} V = {} & a_2 - a_4\, x - a_5\, z - 0.5\, a_8\,(x^2 + \alpha z^2) \\ & - 0.5\, a_{10}\,(x^2\, z + (\alpha z^3)/3) + a_{11}\, y + a_{12}\, xy \\ & + a_{13}\, yz + a_{14}\, xyz - 0.5\, a_{17}(\, z^2 + x^2) \\ & - 0.5\, a_{18}\,(xz^2 + (\alpha x^3)/3) + 0.5\, a_{19}\, z + a_{20}\, xz \\ & + 0.5\, a_{23}\, x \end{aligned} \tag{5b}$$

$$\begin{aligned} W = {} & a_3 + a_5\, y - a_6\, x - 0.5\, a_9\,(x^2 + (\alpha y^2)/3) \\ & - 0.5\, a_{10}\,(x^2 y + (\alpha y^3)/3) - 0.5\, a_{13}\,(\, y^2 + \alpha x^2) \\ & - 0.5\, a_{14}\,(xy^2 + (\alpha x^3)/3) + a_{15}\, z + a_{16}\, xz + a_{17}\, yz \\ & + a_{18}\, xyz + 0.5\, a_{19}\, y + 0.5\, a_{21}\, x + a_{22}\, xy \end{aligned} \tag{5c}$$

3.2 Automatic evaluation of the matrix [K_0]

The evaluation of the elementary stiffness matrix passes by the evaluation of the following expression:

$$K_e] = [A^{-1}]^T\, [K_0]\, [A^{-1}] \tag{6}$$

With

$$[K_0] = \iiint_V [Q]^T\, [D]\, [Q]\, dx.dy.dz \tag{7}$$

And $[B] = [Q]\,[A^{-1}]$

The classic strain matrix is [B], the matrix [A] and its inverse can be estimated numerically, one realizes that the evaluation of the integral (7) becomes the key of the problem. The element shape is regular, numerical integration is reduced to an analytical integration.

3.3 Mechanical characteristics of the fictitious material

The matrix (6) is a modified form (fictitious material) of the material matrix properties by introducing the plane stress constants and a corrective coefficient of transverse shearing (TS) noted K. Where:

K= $\pi^2/12$ in Uflyand-Hencky-Mindlin's theory

K= 5/ 6 in Reissner's theory and ν is the Poisson's ratio

$$[D] = D_1 \begin{bmatrix} 1 & \nu & 0 & 0 & 0 & 0 \\ & 1 & 0 & 0 & 0 & 0 \\ & & D_2 & 0 & 0 & 0 \\ & & & D_3 & 0 & 0 \\ & & & & KD_3 & 0 \\ & & & & & KD_3 \end{bmatrix} \quad (8)$$

where $D_1 = \frac{E}{(1-\nu^2)}$; $D_2 = \frac{(1-\nu)^2}{(1-2\nu)}$; $D_3 = \frac{(1-.\nu)}{2}$

4 NUMERICAL EXPERIMENTS

The precision of the present element is estimated through a series of standard tests limited to simple but self-important applications to show the interest of the strain model. Table 1 gives the details of the pathological tests conducted and also the corresponding figure numbers and table numbers point to the configuration and results, respectively. It is to note that other tests concerning especially the displacements calculations were established for the SBH8, SBBM8 and SBP8C [10, 12] and proved the robustness of these last ones. We quote, constant bending moment patch test, out-of-plane patch test and constant twisting moment patch test for plates.

Table 1: Numerical experiments

Test no	Figures	Type of test	Type of loading	Results
1	Fig.2	Cantilever beam under pure bending	Bending	Table 3
2	Fig.3	Two-element cantilever	Concentrated load ν=0	Table 4
3	Fig.3	Two-element cantilever	Concentrated load ν=0.3	Table 5
4	Fig.4	Single element aspect ratio sensitivity test	Bending	Table 6
5	Fig.5	Cantilever bar subjected to extensional load	Extensional	Table 7
6	Fig.6	Convergence test of moments	Bending-Twisting	Fig.7-10
7	Fig.6	Effect of the aspect ratio on the moment	Bending-Twisting	Fig.11-14

4.1 Eigenvalues

Let us consider the parallelepiped finite element of dimensions 2a x 2b x 2c (Fig.1). We computed eigenvalues of the elementary stiffness matrix [Ke], and found the expected six zero eigenvalues (Table 2) that correspond to rigid body motion and 18 positive eigenvalues that correspond to straining modes. This element does not exhibit extra zero energy modes.

Table 2: Eigenvalues for the SBP8 element

Cases	*v*	*E*	*a*	*b*	*c*	*N*
1st	0,3	10,92	1/2	1/2	1/2	6
2nd	0,3	10,92	1/2	1	1	6
3rd	0	10,92	1/2	1/2	1/2	6
4th	0	10,92	1/2	1	1	6

4.2 Cantilever beam under pure bending

A single-element is subjected to a pure bending load applied as portrayed in Fig.2. The cantilever is of dimensions 10x1x1, the material modulus E and Poisson's ratio ν are 10^6 and 0.0. The elegance of SBP8 can be observed in Table 3, in which the vertical deflections are listed.

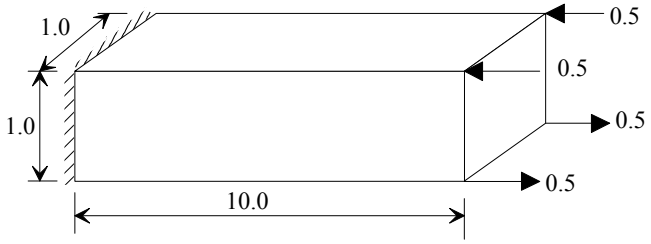

Figure.2: Cantilever beam under pure bending

Table 3: Cantilever beam under pure bending

	W
FI*	$0.11764.\ 10^{-4}$
FCB*	$0.60000.\ 10^{-3}$
SBP8	$0.60000.\ 10^{-3}$
Theory	$0.60000.\ 10^{-3}$

4.3 Two-element cantilever subjected to concentrated transverse tip load

a/ Case 1 (v=0). This problem is considered by Chandra and Prathap's FCB element [15]. A two element cantilever is subjected to concentrated transverse tip load as shown in Fig.3. The cantilever is of dimensions 10x1x1 and the elastic properties are taken as E= 10^6 and ν=0.0. The tip

deflections W and the normal stress σ_{xx} on the top surface at the root and shear stress τ_{xz} at the root are given in Table 4. The analytical solution is calculated by using the formula given in Reference [16]. Predictions of the SBP8, FC, FCB and PN30 yield close results which are superior to FI element.

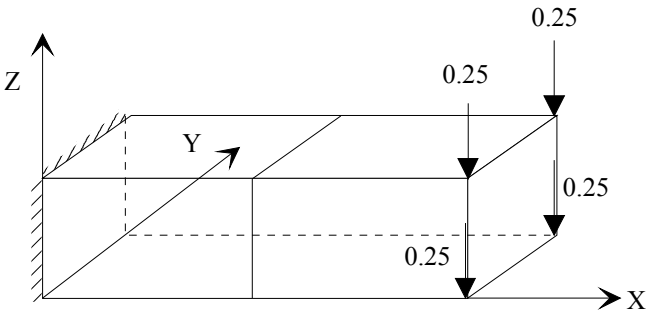

Figure.3: Two-element cantilever under transverse tip load

Table.4: Tip deflections and root stresses for two-element cantilever

	W	σ_{xx}	τ_{xz}
FI*	0.298×10^{-3}	3.33	5.84
FC*	0.378×10^{-2}	45.00	1.00
FCB*	0.378×10^{-2}	45.00	1.00
PN30**	0.378×10^{-2}	45.00	1.00
SBP8	0.377×10^{-2}	45.00	1.00
Theory	0.400×10^{-2}	45.00	1.00

Table 5: Tip deflections two-element cantilever subjected to concentrated transverse tip load

	W
FI*	0.263×10^{-3}
FC*	0.320×10^{-2}
FCB*	0.362×10^{-2}
PN30**	0.360×10^{-2}
CSA/NASTRAN (8601)	0.320×10^{-2}
ASKA 8.5	0.293×10^{-2}
SBP8	0.364×10^{-2}
Theory	-

* Source: [13]. ** Source: [14].

b/ Case 2 (ν=0.3). To examine the nature of Poisson's ratio stiffening, the calculation with ν=0.3 is conducted. Table 5 shows the deflections obtained with the various eight-nodded brick elements from two major general-purpose programs, the CSA/NASTRAN and ASKA 8.5 programs. The SBP8 is free from both shear locking and Poisson's locking.

4.4 The single-element aspect ratio sensitivity test

A very severe test is proposed [18] for any solid element undergoing pure bending without parasitic shear or Poisson's ratio stiffening. We consider a single eight-node brick element, as shown in figure.4, with 2b=0.06m, 2c=0.06m and L varied so that aspect ratios from one to eight are covered. The elastic proprieties are $E=207 \times 10^9 N/m2$, ν=0.25 and $G=82.8 \times 10^9 N/m^2$. A constant bending moment field of M=1656Nm is applied in the form of a pair of concentrated couples at the four nodes on the free end and a fifth force is applied in the direction of the unconstrained freedom on the face x=0. Table 6 presents' results for the SBP8 element and compares these with the values obtained from identical tests with the eight-node brick elements from some well-known general purpose finite element packages. It is clear that the SBP8 solid element gives exact results for Robinson's single element test [18].

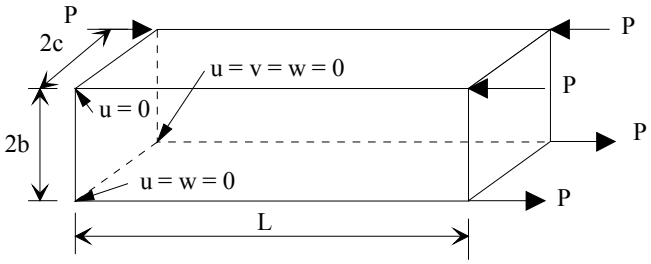

Figure 4: Single-element test for aspect ratio sensitivity of solid element.

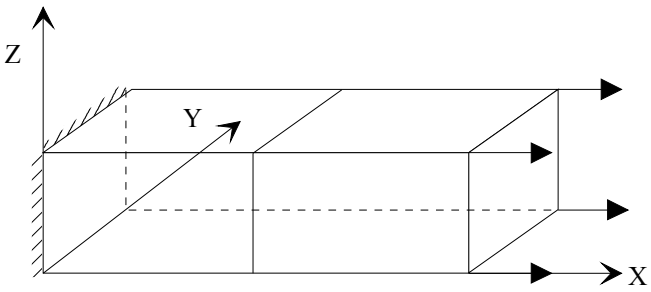

Figure 5: Extensional response of two element bar.

Table 6: Results for the single-element test for aspect ratio sensitivity

Elements	Displacement parameter	Aspect ratio L/2b			
		1	2	4	8
FC*, CSA/NASTRAN, ASKA 8.5	α	3.125	6.25	12.5	25.0
	β	-1.0417	-1.0417	-1.0417	-1.0417
	γ	3.125	12.5	50.0	200.0
PN340**	α	-	-	-	-
ANSYS, PN5X1***	β	-0.833	-0.833	-0.833	-0.833
	γ	-	-	-	-
FCB*		As theory			
MSC/NASTRAN		As theory			
SBP8		As theory			
Theory	α	3.333	6.666	13.333	26.666
	β	-0.833	-0.833	-0.833	-0.833
	γ	3.333	13.333	53.333	213.33

U=α x 10-6 ; V=β x 10-6 ; W=γ x 10-6 Source: [15]. ** Source: [14]. *** Source: [19].

Table 7: Axial extension of the bar as ν→0.5

ν	**FC***	**FI***	**SBP8**
0.0	0.1000×10^{-5}	0.1000×10^{-5}	0.10000×10^{-5}
0.45	0.8876×10^{-6}	0.7735×10^{-6}	0.96741×10^{-6}
0.495	0.8607×10^{-6}	0.3106×10^{-6}	0.95943×10^{-6}
0.4995	0.8577×10^{-6}	0.4551×10^{-6}	0.95856×10^{-6}
0.49995	0.8574×10^{-6}	0.4775×10^{-6}	0.95848×10^{-6}
0.499995	0.8574×10^{-6}	0.4800×10^{-6}	0.95847×10^{-6}
0.4999995	-	-	0.95847×10^{-6}
0.49999999995	-	-	0.95847×10^{-6}

* Source: [15].

4.5 Cantilever bar subjected to an extensional load

To demonstrate the effectiveness of the SBP8 element in incompressible situation, we consider the response of a two-element bar to an extensional load applied as shown in Fig.5. The bar is of dimensions 10x1x1 and $E=10^6$.

Strength of material approximation predicts an axial extension $U = 1 \times 10^{-6}$. The finite element results are shown in Table 7 as ν varied from 0.0 to 0.4999999995. It is found that the SBP8 performs very well under near incompressibility.

4.6 Moment convergence tests for square plate

The next set of tests concerns a laterally loaded square plate; it has become a *de facto* standard test and has been seen frequently in the technical literature [20]**.** In this series of tests, a quarter of plate (Fig.6) is modeled and tested for a uniformly distributed load. These tests are carried out for both a simply supported plate and clamped plate. We display the solutions obtained in the form of graphs for different meshes.

Figures 7-8 show the moments results obtained from a bending and twisting convergence test for a simply supported plate, with a uniformly distributed load. Figures 9-10 refer to the solution also obtained for the same experiment, but this time with clamped conditions. Moment results are compared with the solution given by the ACM element [16][17].

These results illustrate stability and good performance of the SBP8 element, whereas the classic element B8 gives bad results (austere locking in transverse shear).

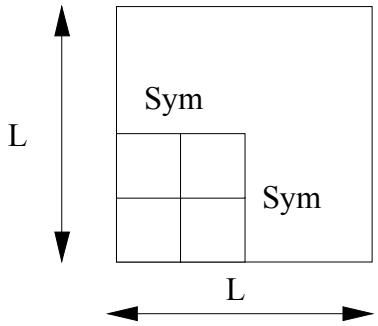

Figure.6: Square Plate for convergence tests.

L=1, t=0.01, E=10.92 , v = 0.3, uniformly distributed load q=1, K=π2/12 (Mindlin's coefficient).

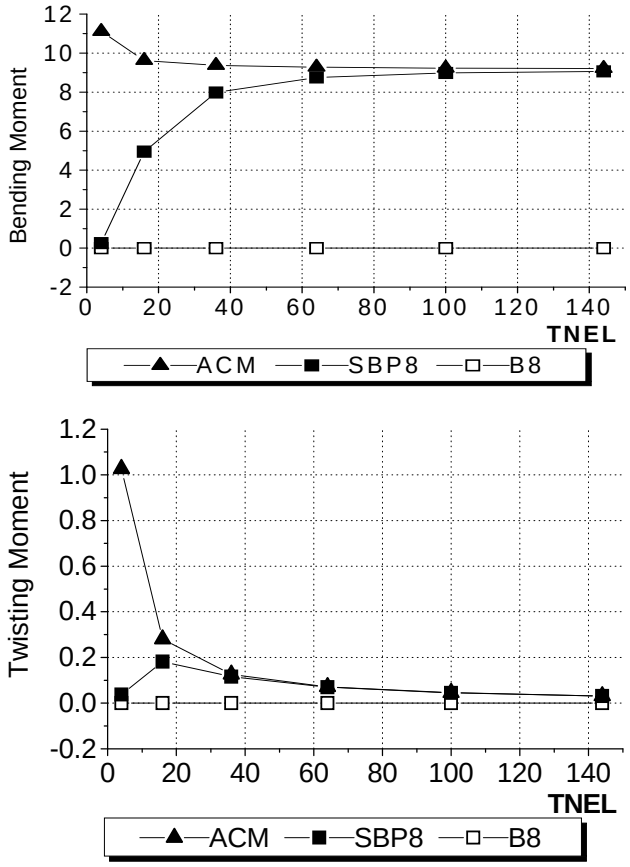

Fig.7-8: Convergence test of the moments (bending-twisting), Simply Supported Plate

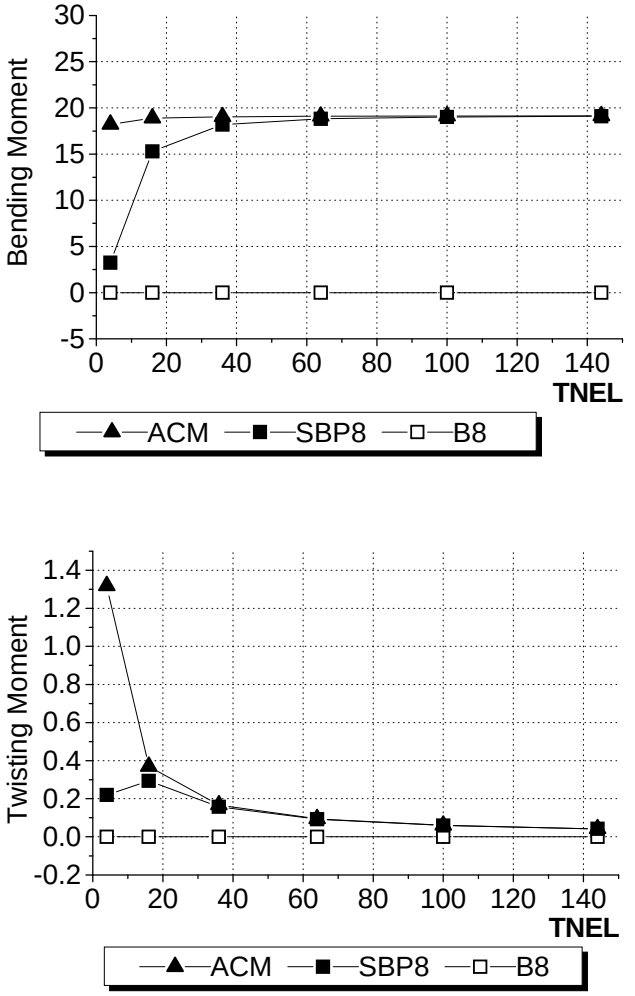

Figure9-10: Convergence test of the moments (bending-twisting), Clamped Plate

4.7 Effect of the aspect ratio on the moments

The effect of the aspect ratio on the moments (bending and twisting) for a square plate taken under different conditions has been studied. We keep sides of the plate constant and vary only their thickness to perform locking tests for length to thickness ratios varying from 2.5 to 100. Figures 11-14 show that the B8 locks due to the presence of excessive shear. The SBP8 shows improved performance, it does not lock for different boundary conditions. Results obtained with the element SBP8 are normalized with regard to the solution given with the ACM element, B8 as in the previous case stays far from the solution

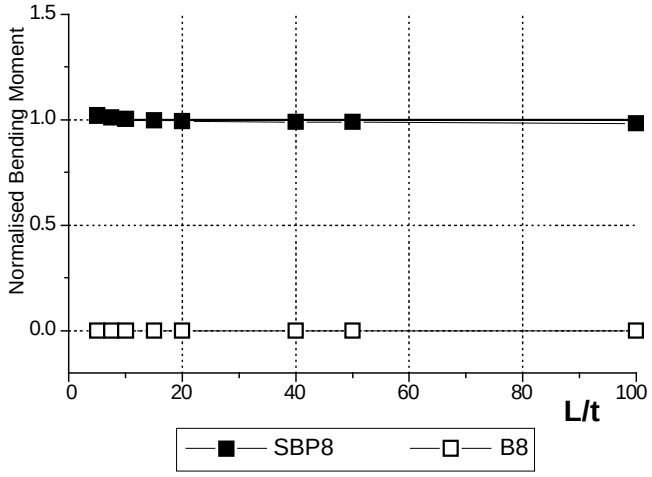

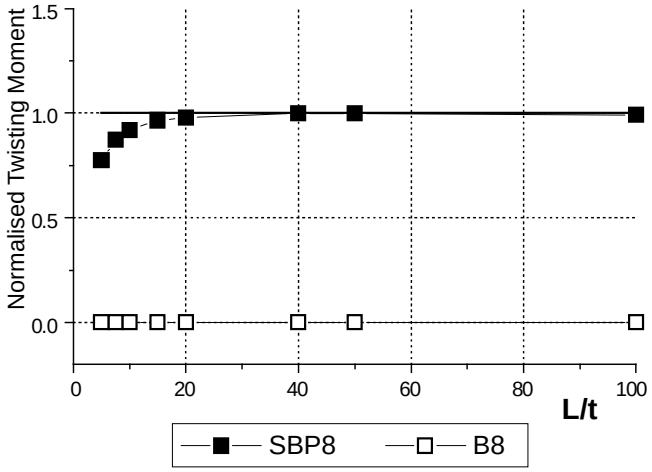

Figure 11-12: Influence of L/t on the bending and twisting moments, Simply Supported Plate

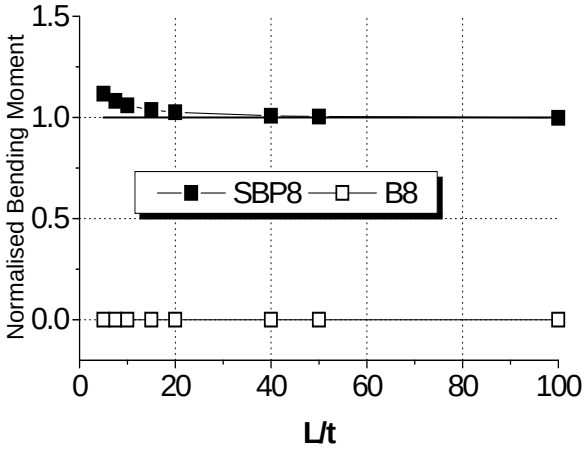

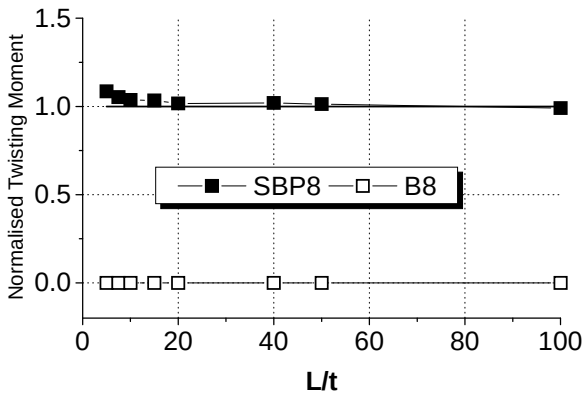

Figure13-14: Influence of L/t on the bending and twisting moments, Clamped Plate

5 CONCLUSION

This study shows that it is essential for 3D strain based elements, to modify the law of behavior for the plate bending calculation. The main improvement is obtained as a result of the use of the plane stress constants. The use of a corrective coefficient of transverse shear gives a supplementary improvement. 3D strain based elements are free from locking. The robustness of the SBP8 element was demonstrated, the plate bending can be very well simulated with this simple element based on the strain model. Finally, this element presents the advantage to be able to take into account easily brusque variation of plate thickness, and to be linked without important modification for three-dimensional structures. The question now, can one generate a new displacement field witch verify the equilibrium and compatibility equations and improve the displacements and moments results. An investigation is currently undertaken on this aspect.

REFERENCES BIBLIOGRAPHIQUES

[1] Ashwell D.G., Sabir A.B. and Roberts T.M., Further studies in the application of curved finite elements to circular arches, *IJMS* Vol. 13, pp. 507-517, 1971

[2] Sabir A.B. and Ashwell D.G., A comparison of curved beam finite elements when used in vibration problems, *Journal of Sound and Vibration*, Vol.18, N°11, pp. 555-563, 1971.

[3] Sabir A.B. A new class of Finite Elements for plane elasticity problems, *CAFEM 7th, Int. Conf. Struct. Mech. InReactor Technology, Chicago*, 1983.

[4] Sabir A.B. and Salhi H.Y., A strain based finite element for general plane elasticity in polar coordinates, *Res.Mechanica* 19, pp. 1-16, 1986.

[5] Belarbi M.T. et Charif A., Nouvel élément secteur basé sur le modèle de déformation avec rotation dans le plan, *Revue Européenne des Eléments Finis*, Vol.7, N04, pp. 439-458, Juin 1998.

[6] Belarbi M.T. et Charif A., Développement d'un nouvel élément hexaédrique simple basé sur le modèle en déformation pour l'étude des plaques minces et épaisses, *Revue Européenne des Eléments Finis*, Vol.8, N^0 2, pp. 135-157, 1999.

[7] Belarbi M.T. Développement de nouveaux éléments finis basés sur le modèle en déformation. Application linéaire et non linéaire. Thèse de Doctorat d'Etat, Université de Constantine 2000 (Algrie)

[8] Maalem T., *Investigation numérique des problèmes de flexion de plaque par un élément fini parallélépipédique basé sur le modèle en déformation*, mémoire de Magistère, Université de Constantine, Algérie, 2002.

[9] M.T.Belarbi & T.Maalem., *A New Parallelepiped Finite Element For Thin and Thick Plates*", ICCES, Vol. 1, 7-8 October 2003, Asyut- Egypt.